

Density changes during the fractional crystallization of basaltic magmas: fluid dynamic implications

R. Stephen J. Sparks¹ and Herbert E. Huppert²

¹ Department of Earth Sciences, University of Cambridge, Cambridge CB2 3EQ, UK

² Department of Applied Mathematics and Theoretical Physics, University of Cambridge, Cambridge CB3 9EW, UK

Abstract. The dynamical behaviour of basaltic magma chambers is fundamentally controlled by the changes that occur in the density of magma as it crystallizes. In this paper the term *fractionation density* is introduced and defined as the ratio of the gram formula weight to molar volume of the chemical components in the liquid phase that are being removed by fractional crystallization. Removal of olivine and pyroxene, whose values of fractionation density are larger than the density of the magma, causes the density of residual liquid to decrease. Removal of plagioclase, with fractionation density less than the magma density, can cause the density of residual liquid to increase. During the progressive differentiation of basaltic magma, density decreases during fractionation of olivine, olivine-pyroxene, and pyroxene assemblages. When plagioclase joins these mafic phases magma density can sometimes increase leading to a density minimum. Calculations of melt density changes during fractionation show that compositional effects on density are usually greater than associated thermal effects.

In the closed-system evolution of basaltic magma, several stages of distinctive fluid dynamical behaviour can be recognised that depend on the density changes which accompany crystallization, as well as on the geometry of the chamber. In an early stage of the evolution, where olivine and/or pyroxenes are the fractionating phases, compositional stratification can occur due to side-wall crystallization and replenishment by new magma, with the most differentiated magma tending to accumulate at the roof of the chamber. When plagioclase becomes a fractionating phase a zone of well-mixed magma with a composition close to the density minimum of the system can form in the chamber. The growth of a zone of constant composition destroys the stratification in the chamber. A chamber of well-mixed magma is maintained while further differentiation occurs, unless the walls of the chamber slope inwards, in which case dense boundary layer flows can lead to stable stratification of cool, differentiated magma at the floor of the chamber.

In a basaltic magma chamber replenished by primitive magma, the new magma ponds at the base and evolves until it reaches the same density and composition as overlying magma. Successive cycles of replenishment of primitive magma can also form compositional zonation if successive cycles occur before internal thermal equilibrium is reached

in a chamber. In a chamber containing well-mixed, plagioclase-saturated magma, the primitive magma can be either denser or lighter than the resident magma. In the first case, the new magma ponds at the base and fractionates until it reaches the same density as the evolved magma. Mixing then occurs between magmas of different temperatures and compositions. In the second case a turbulent plume is generated that causes the new magma to mix immediately with the resident magma.

Introduction

Density is a physical property of fundamental importance in many magmatic processes because the detailed changes of liquid density that occur during fractional crystallization can have controlling influence on the dynamical processes of magmatic differentiation. Several recent investigations have shown how selective removal of components from a fluid due to crystallization can lead to important convective phenomena. Cooling of a closed system, from either the sides, roof or floor can lead to compositional and thermal stratification from an initially homogeneous fluid and to development of double-diffusive layering (Chen and Turner 1980; McBirney 1980; Turner and Gustafson 1981). Replenishment of a container can also lead to compositional and thermal stratification and to mixing between fluids of different compositions (Huppert and Sparks 1980a, b; Irvine 1980; Huppert and Turner 1981; Huppert et al. 1982). These effects of crystallization and replenishment will have a fundamental influence on the compositions of erupted magma and on the character of the layered plutonic rocks which eventually fill the chamber.

In this paper the changes in magma density due to fractional crystallization of the major crystalline phases found in mafic and ultramafic rocks are considered. The concept of *fractionation density* is introduced, which is the density of those components in the fluid which are being selectively removed by crystallization. Fractionation density is calculated as the ratio of the gram formula weight to molar volume of the chemical components in the melt phase that are incorporated into the fractionated crystalline phases. Graphs of fractionation densities are presented for the major minerals crystallized from basaltic magmas. Morse (1969) introduced essentially the same concept, which he called liquid mineral density. The concept is considered to

be useful in understanding general properties of the variation of melt density during fractional crystallization.

The implications of the density changes during fractional crystallization for the fluid dynamic behaviour of magma chambers are considered. General fluid dynamical models of the evolution of both closed-system and open-system basaltic magma chambers are presented based on experimental and theoretical understanding of convection in crystallizing systems.

Density variations in basaltic magmas

Density determinations

Bottinga and Weill (1970) developed an empirical method for determining the density of silicate melts as a function of bulk composition and temperature. They and others (Nelson and Carmichael 1979; Bottinga et al. 1982; Mo et al. 1982) determined the partial molar volume and expansion coefficients of the major oxide components in a variety of two-component and three-component systems over a range of temperatures.

An important assumption in applying these data to natural silicate systems is that the partial molar volume of a component is independent of bulk composition. Nelson and Carmichael (1979) show that, within the experimental standard errors of the partial molar volume determinations (typically $\ll 2\%$), this is a reasonable assumption except for Al_2O_3 . The expression for calculating density is given by Bottinga and Weill (1970) as

$$\rho = \frac{\sum_i x_i M_i}{\sum_i x_i V_i} \quad (1)$$

where x_i , M_i and V_i are respectively the mole fraction, the molecular mass and the partial molar volume of the i^{th} component.

In all our calculations the partial molar volume and expansion coefficient data of Nelson and Carmichael (1979) were used with the exception of Al_2O_3 and Fe_2O_3 . For Al_2O_3 we have estimated the composition-dependent partial molar volume and expansion coefficient from the empirical expressions given in Bottinga et al. (1982). For Fe_2O_3 we have used the measurements of partial molar volume and expansion coefficient in Mo et al. (1982).

In all our calculations a pressure of one atmosphere was assumed. The compressibility of basaltic magma has only been determined in a few experiments (Fujii and Kushiro 1977; Kushiro 1982). However, pressure effects are not considered to influence the conclusions reached in this paper because, as will emerge below, it is density differences that matter rather than absolute values of density in determining the processes of fractionation. The relative density variation of two closely related basaltic melts of different composition does not change significantly as pressure is increased, at least within the pressure range of upper crustal magma chambers (Kushiro 1982).

There are a number of errors associated with the determination of density in silicate melts. These errors arise from experimental uncertainties, from inaccuracies in the chemical analyses of samples and from uncertainties concerning the oxidation state of iron. As rather small density differences will be found to have profound effects on the dynam-

Table 1. Comparison of measured and calculated densities of basaltic and other silicate melts in g cm^{-3}

Composition	Source	T(°C)	2 σ (%)	ρ (measured)	ρ (calculated)
Kil 2	1	1,400	0.80	2.709	2.698
004	2	1,400	0.84	2.639	2.645
Vil Haven	3	1,250	0.90	2.640	2.648
Diabase*					
GOB*	4	1,240	0.87	2.685	2.680
CRB*	4	1,390	0.93	2.590	2.589
CRB**	4	1,390	0.79	2.670	2.652
SLS**	4	1,400	0.94	2.950	2.907
005	2	1,400	0.98	2.762	2.733
006	2	1,400	1.15	2.859	2.824
009	2	1,400	1.46	2.845	2.838
003	2	1,400	1.60	2.931	2.967
Synthetic	3	1,391	1.20	2.671	2.660
diopside					
Akermanite	3	1,458	1.22	2.724	2.724
Plagioclase	3	1,480	1.10	2.519	2.500
(An ₇₀)					

Sources of data: (1) Nelson and Carmichael (1979); (2) Mo et al. (1982); (3) Dane (1941); (4) Murase and McBirney (1973)

* All Fe as Fe_2O_3 ** All Fe as FeO

ics of magma chambers an assessment of the magnitude of the errors associated with calculations using Eq. (1) is essential.

Table 1 lists the few available density measurements of basaltic melts and some iron-rich basic melts. Density measurements on melts corresponding to specific mineral compositions are also listed. The densities of these melts at specified temperatures were calculated using Eq. (1) and are also listed. The measured and calculated densities are plotted against each other in Fig. 1. The experimental errors on the measurements are estimated by the various authors as generally better than 1%. For each calculated density the 2σ error is listed as a percentage of the density. These values were calculated using the standard error data on partial molar volumes (Nelson and Carmichael 1979; Mo et al. 1982) and the expression

$$\sigma = \sum_{i=1}^N \sqrt{x_i^2 \sigma_i^2} \quad (2)$$

Six of the samples have compositions corresponding to natural basaltic rocks (CRB, GOB, Kil2, Vil Haven diabase, 004 and SLS). For these samples agreement between the measured and calculated densities is better than 0.5% (Fig. 1) except the synthetic lunar sample (SLS). For the iron-rich compositions investigated by Mo et al. (1982) agreement is not as good with the density values differing by as much as 1.3%. The densities of CRB, GOB and the Vil Haven diabase were calculated assuming that all iron was present as Fe_2O_3 , since the density determinations were made in air. This assumption is supported by the observation that there is a marked discrepancy between measured and calculated density for GOB if it is assumed that all iron is present as FeO (Fig. 1). Murase and McBirney (1973) also measured the density of sample CRB under reducing conditions. The measured density was much higher than under oxidising conditions and agrees closely with

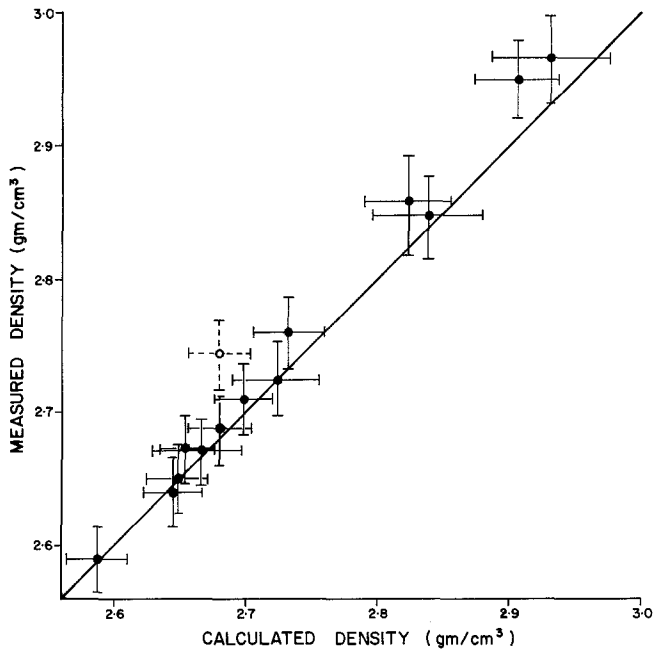


Fig. 1. Plot of calculated versus measured densities for basaltic melts and melts of mineral phases. The 2σ error bars are shown as listed in Table 1, which also gives sources for the data. The open circle shows the position of sample GOB assuming all iron as FeO

the calculated density assuming iron to be present as FeO (Table 1).

The available data indicate that density calculations on common basaltic melts have an accuracy of about 0.5%. Unfortunately the range of densities among basaltic magmas related by fractional crystallization can often be less than 2% (Sparks et al. 1980; Stolper and Walker 1980). Thus, even if basalt compositions are known from field data or experiments, small differences in density calculated with equation (1) cannot be considered meaningful. On the other hand a difference of 0.5% in density between two melts of different composition can have profound dynamic effects and can lead to a variety of important convective phenomena (Sparks et al. 1983). For comparison the temperature change required to produce a 0.5% decrease in density of a basalt melt is approximately 250° C.

Fractionation density

A melt which consists initially of N components with mole fractions x_j ($j=1,2,3\dots N$) has a density

$$\rho_i = \frac{\sum_{j=1}^N x_j M_j}{\sum_{j=1}^N x_j V_j} \equiv \bar{M}/\bar{V}, \quad (3)$$

where \bar{M} is the gram formula weight and \bar{V} is the partial molar volume of the melt. From the initial melt, an amount of fractional crystallization occurs, removing minerals that consist of components in the mole fraction ratio r_j ($\sum r_j = 1$). A parameter ρ_c can be defined which will be termed the *fractionation density* and is given by

$$\rho_c = \frac{\sum r_j M_j}{\sum r_j V_j} \equiv M_c/V_c. \quad (4)$$

For example, if the mineral is forsterite

$$\rho_{(Mg_2SiO_4)} = \frac{\left(\frac{1}{3}\right) M_{SiO_2} + \left(\frac{2}{3}\right) M_{MgO}}{\left(\frac{1}{3}\right) V_{SiO_2} + \left(\frac{2}{3}\right) V_{MgO}} \quad (5)$$

A value of ρ_c can be readily calculated for any combination of minerals crystallizing in any desired proportion. The *fractionation density* can be defined as the density of the components of the fluid being selectively removed by fractional crystallization. It is important to emphasize that this is a fictive parameter and is not related to the solid densities of the minerals. The reason for introducing it is to enable general statements to be made on the changes of melt density that are caused by fractionation of different mineral assemblages.

Suppose a molar fraction X of crystallizing minerals is removed from the initial melt to form a final melt. The density of the final melt can be shown to be

$$\rho_f = \frac{\sum (x_j - X r_j) M_j}{\sum (x_j - X r_j) V_j} \quad (6)$$

which can be rearranged to give

$$\rho_f = \frac{\rho_i \left(1 - \frac{\rho_c}{\rho_i} \frac{\bar{V}_c}{\bar{V}_i} X\right)}{\left(1 - \left(\frac{\bar{V}_c}{\bar{V}_i}\right) X\right)} \quad (7)$$

It is clear from Eq. (7) that if the density contribution (ρ_c) of the components being removed by fractional crystallization is greater than the initial melt density (ρ_i) then the magma density will decrease during fractional crystallization. If the value of ρ_c is less than ρ_i the magma density will increase during fractional crystallization.

In Fig. 2 the values of fractionation density are plotted against composition for the major solid-solution series of minerals found in basaltic magmas: olivine, clinopyroxene, orthopyroxene and plagioclase. The fractionation densities of each solid solution series at 1,200° C and 1,400° C have been calculated to show the small effect of temperature variation at a fixed mineral composition. Also shown on the diagram are the density ranges of common basaltic liquids. The fractionation densities of olivine and, in most cases, the pyroxenes are greater than common basaltic magmas and will therefore cause a decrease in magma density during fractionation. The fractionation density of plagioclase is less than most common basalts and so density will normally increase during fractional crystallization of basalt if plagioclase is the only mineral forming. The measured densities of pure melts of diopside, labradorite (An_{70}) and akermanite are compared with their fractionation densities in Table 1, showing that there is close agreement, well within the 2σ error bar shown in Fig. 2. Melts of the same composition as the fractionating minerals cannot of course exist at the typical temperatures of basaltic magma. We emphasize that the fractionation density as defined in Eq. (4) and (7) relates only to chemical components in the melt.

When more than one phase is involved in crystallization, the value of the fractionation density is simply the weighted sum of the fractionation densities of the involved phases. The fractionation densities of assemblages crystallizing in cotectic proportions from basaltic magmas have been calculated to illustrate the principle. Enough is now known about

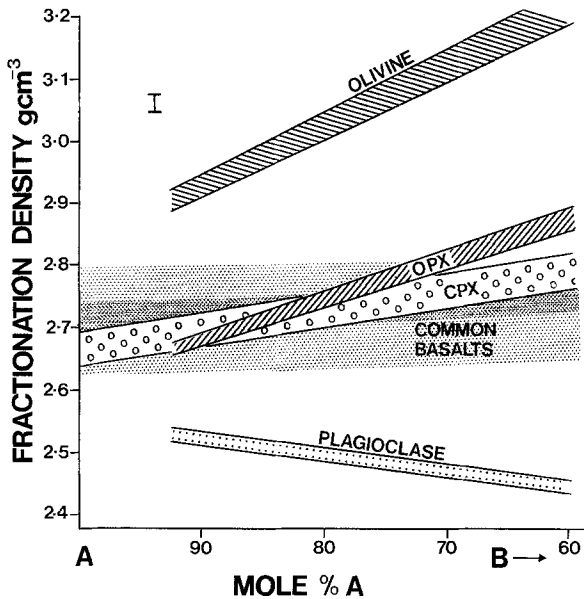


Fig. 2. Fractionation densities of olivine, orthopyroxene, clinopyroxene and plagioclase plotted against composition. The components A and B are separately defined for each mineral: olivine $A = \text{Mg}_2\text{SiO}_4$ and $B = \text{Fe}_2\text{SiO}_4$; orthopyroxene $A = \text{MgSiO}_3$ and $B = \text{FeSiO}_3$; clinopyroxene $A = \text{CaMgSi}_2\text{O}_6$ and $B = \text{CaFeSi}_2\text{O}_6$; plagioclase $A = \text{CaAl}_2\text{Si}_2\text{O}_8$ and $B = \text{NaAlSi}_3\text{O}_8$. For each mineral fractionation densities have been calculated at $1,200^\circ\text{C}$ (upper line) and at $1,400^\circ\text{C}$ (lower line). The density range of common basaltic magmas is indicated and a typical 2σ error bar for the density estimates is shown in the top left hand corner

the phase equilibria of basaltic magmas to estimate the approximate proportions of minerals crystallizing on cotectic surfaces at 1 atmosphere (Irvine 1970). Table 2 lists some commonly observed combinations of minerals and their cotectic proportions. The proportions have been slightly simplified from those suggested by McCallum et al. (1980).

The fractionation densities of cotectic assemblages will depend on the compositions of the minerals and on temperature. Fig. 3 shows contours of fractionation density at $1,200^\circ\text{C}$ for each cotectic assemblage as a function of mineral compositions. For the graphs involving clinopyroxene we have used a constant value of fractionation density of 2.75 g cm^{-3} for the clinopyroxene in order to simplify the presentation. In Fig. 3 the fractionation densities of minerals which are naturally found in association in layered intrusions and some lavas are plotted to delineate the regions of most interest.

An interesting feature of Fig. 3 is that, in all cotectic assemblages involving plagioclase, the natural spread of compositional associations in individual intrusions is almost parallel to the fractionation density contours. This implies that there is little variation in fractionation densities of each cotectic assemblage during differentiation. These ranges are listed in Table 2.

Density variations during fractionation

Knowledge of the liquid density and its variation as fractionation proceeds are necessary to predict many of the features of the resulting dynamics and structure in a magma chamber. The idea that the density of basaltic magma varies during fractional crystallization has been pointed out by Sparks et al. (1980) and Stolper and Walker (1980). These

Table 2

Rock type	Olivine	Plag	Cpx	Opx	Fractionation density
Troctolite	30	70	—	—	2.64–2.69
Norite	—	65	—	35	2.59–2.61
Olivine gabbro	10	55	35	—	2.62–2.65
Gabbronorite	—	55	25	20	2.59–2.63

authors proposed that olivine crystallization produced a decrease in melt density whereas plagioclase crystallization produced an increase in melt density. However, the various methods used to calculate melt density variation during fractionation were unsatisfactory. Sparks et al. (1980) used the densities of natural basaltic glasses to show the presence of a density minimum. These glasses, however, were probably related to one another not only by fractional crystallization, but also by magma mixing (Bryan 1979; Walker et al. 1979) and partial melting. Stolper and Walker (1980) calculated densities on glass compositions from two experimental studies (Bender et al. 1978; Walker et al. 1979). In both studies errors in probe analyses can cause scatter which could mask subtle density variation. In addition, the experiments of Walker et al. (1979) involved a composition with plagioclase on the liquidus and the melt had evidently been generated by magma mixing. The density changes observed during the crystallization of such a composition would not be truly representative of the course of fractional crystallization.

The density changes observed by Sparks et al. (1980) and Stolper and Walker (1980) were not large (typically of order 1–2%), and consequently some doubt has been expressed about the significance of these changes. Use of the fractionation density concept supports the ideas of Sparks et al. (1980) and Stolper and Walker (1980). The differences in liquid density and fractionation density are often much larger than the errors involved in the calculations (Fig. 2). Thus the change in density accompanying an increment of crystallization can be confidently predicted.

The general form of density variation with fractionation of ultrabasic and basic magmas can also be predicted using the fractionation density. Our considerations will be based on the density curve such as the one shown in Fig. 4. The graph shows the typical variation of density with differentiation in anhydrous basaltic magmas using $(\text{Mg}/\text{Mg} + \text{Fe})$ content as a convenient differentiation index measure (Sparks et al. 1980; Stolper and Walker 1980). No specific scale appears on the figure since the exact dependence of density on temperature and composition will vary from system to system depending upon the bulk composition of the primitive magma and the values of the intensive parameters during differentiation such as pressure, $f\text{O}_2$ and volatile content.

The general shape of the density vs composition plot shows an initial decrease in liquid density to a minimum point A, followed by an increase to a maximum density at B. This pattern will occur in most common basaltic magmas except perhaps those with high H_2O contents. The initial decrease in liquid density of primitive magmas such as komatiites and picritic basalts reflects the fact that the calculated fractionation density is initially greater than the magma density. This occurs not only when olivine is the

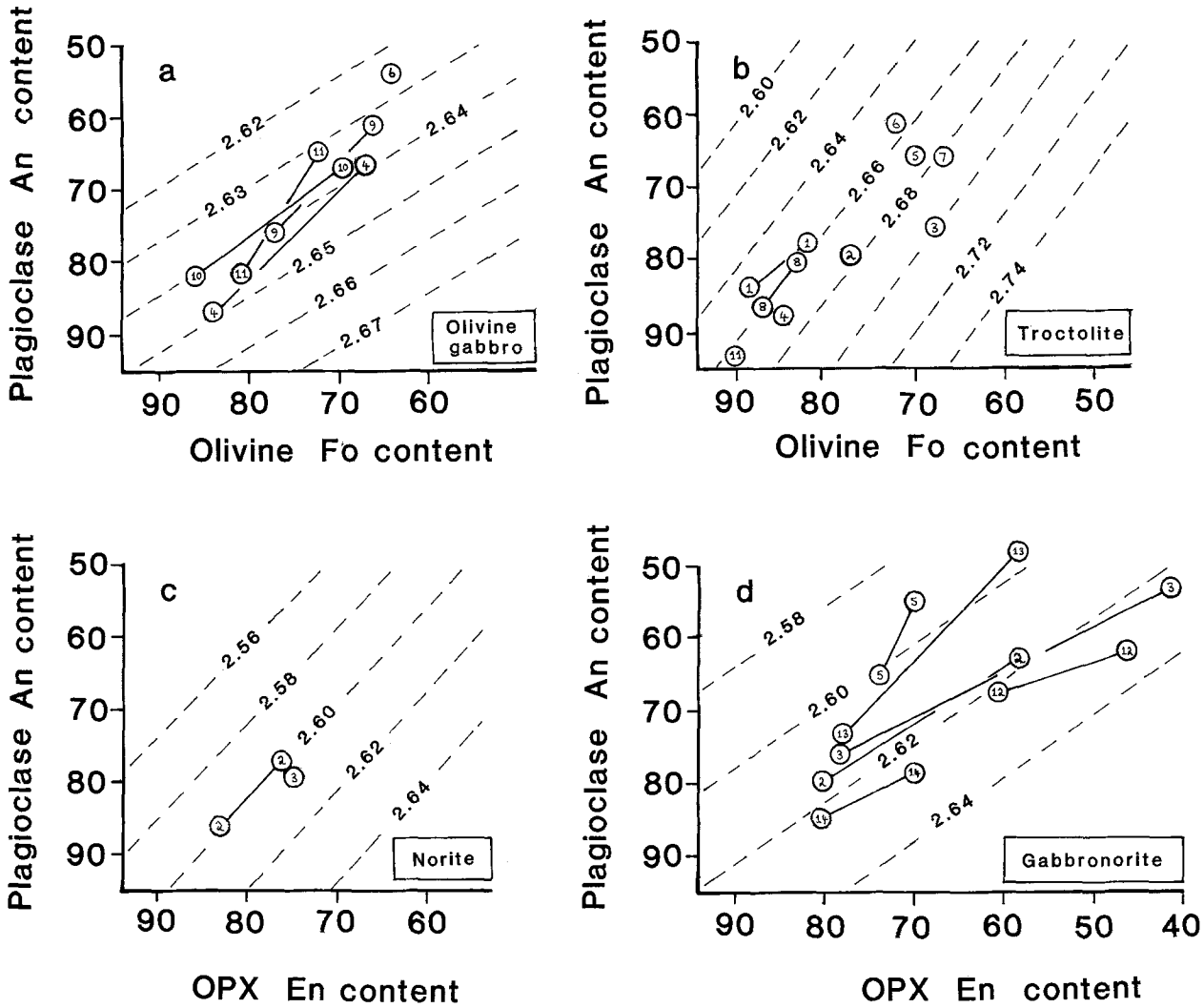


Fig. 3. Fractionation densities at 1,200° C of cotectic assemblages in basaltic systems. The proportions of minerals for each assemblage are given in Table 2. The compositions of naturally-occurring assemblages from various layered intrusions and lava suites are plotted. Contours are of fractionation density in $g\ cm^{-3}$. Legend: (1) Dufek intrusion, Antarctica; (2) Stillwater complex, Montana; (3) Bushveld Complex; (4) Rhum intrusion, N.W. Scotland; (5) Kaeravaen intrusion, East Greenland; (6) Kiglapait intrusion, Labrador; (7) Skaergaard intrusion, East Greenland; (8) phenocrysts in mid-ocean ridge basalts of the FAMOUS area; (9) Kap Edvard Holm, Greenland; (10) Oman ophiolite, plutonic section; (11) Cuillin gabbro, Skye; (12) Inch Intrusion, Scotland; (13) Hartley Complex, Great Dyke, Zimbabwe; (14) Kapalagulu intrusion, Tanzania

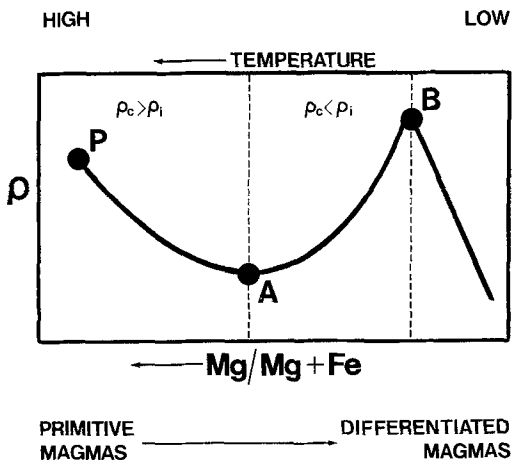


Fig. 4. Schematic relationship between magma density and $(Mg/Mg+Fe)$ for basaltic melts related to one another by fractional crystallization

fractionating phase, but also when olivine-pyroxene assemblages or olivine-plagioclase assemblages with insufficient plagioclase to make ρ_c less than ρ_l are being fractionated. When plagioclase becomes a major component the fractionation density often decreases well below the typical densities of basaltic magma (Table 2) and causes an increase in the liquid density vs composition trend and an associated density minimum. This minimum density occurs in mid-ocean ridge basalts at MgO values typically between 7 and 10% (Sparks et al. 1980). In highly differentiated basalts the trend can reverse yet again as ferromagnesian phases become iron-rich and iron-rich phases such as ilmenite appear, resulting in the increase of density. In Fig. 4 the density curve has been drawn so that the density at the maximum point B exceeds the density of the primitive magma. This need not necessarily be so and our discussion below will consider both what happens in this case and when the local density maximum is less than that of the primitive magma.

The relative densities of the primitive magma, the mini-

imum A and the maximum B will depend on the many factors that control the compositions of partial melts of the mantle and the paths of fractional crystallization in the crust. We can envisage, for example, a system with a parental melt with $\text{MgO} \sim 12\%$, such as that proposed by Presnall et al. (1979), that would be close to the density minimum and would therefore be lighter than most differentiated magmas. Alternatively, highly magnesian picrite or komatiite will generally be denser than derived magmas produced by fractional crystallization.

The kind of density versus fractionation curve shown in Fig. 4 is most applicable to anhydrous tholeiitic basalt systems. Other kinds of basic magma involving different phases and volatile contents could show more complicated patterns. Two general conclusions can be made relevant to all magma systems. First, gradual changes in slope can be expected as the mineral compositions and fractionation densities change during fractionation. Second, sudden changes in slope of density versus composition curves can be expected when new phases join old phases or when a phase reacts with the liquid (see Grove et al. 1982). In many cases maxima and minima can be expected.

Fluid dynamical implications

In assessing the fluid dynamical behaviour of magma chambers it is important to consider the relative contributions of temperature and composition to melt density (Huppert and Sparks 1984). In the process of fractional crystallization an increment of crystallization is associated with a temperature change and a change of melt composition. The ratio of the density changes associated with the thermal and compositional effects can be expressed as

$$Q = \beta \Delta S / \alpha \Delta T, \quad (8)$$

where β is the coefficient of expansion due to compositional change, ΔS is the change in melt composition, α is the coefficient of thermal expansion and ΔT is the temperature change. Application of the fractionation density concept to fractional crystallization models shows that compositional effects usually dominate over thermal effects in determining how melt density changes. Q typically has values between 1 and 5. Thus, for example, magma density decreases during fractionation of olivine from a picritic basalt ($Q \sim 4.5$) despite the associated temperature decrease.

Differentiation of basaltic magma has traditionally been attributed to settling of crystals. However, a plausible alternative mechanism involves the separation of liquid from solid by convection. In a quiescent fluid rejection or incorporation of solute results in an exponential concentration profile in a thin film adjacent to the growing crystal. Such a film develops compositional and density gradients and the fractionated fluid can convect away from its point of origin. Sparks et al. (1984) have calculated that in basaltic magma chambers such films should be unstable and therefore continual convection of differentiated fluid should occur away from growing crystals. This process is termed *convective fractionation* and has been illustrated in crystallization experiments with aqueous solutions (Turner and Gustafson 1981; Huppert and Sparks 1984). In estimating the effects of convective fractionation it is necessary to know the effect of crystallization on the local density of

melt. Thus if convective fractionation proves to be an important mechanism of differentiation, knowledge of fractionation densities will be useful.

Another cause of compositional diversity in basaltic magmas and layered intrusions is replenishment of a magma chamber by an influx of new magma. The contrast between the new magma and resident magma arises largely from their compositional difference. As indicated in previous studies (Sparks et al. 1980; Huppert and Sparks 1980b) the fluid dynamic behaviour of the chamber will depend fundamentally on the magnitude and sign of the density contrast and on the effects on density of crystallization during the interaction of the magmas. A knowledge of how density changes with fractional crystallization will be essential to understanding these processes.

To illustrate the fluid dynamic implications of the density calculations, the evolution of closed-system and open-system magma chambers is now discussed in terms of the density changes associated with fractionation and recent theoretical and experimental studies of convection in multi-component, crystallizing systems (Sparks et al. 1984; Huppert and Sparks 1984). The fluid dynamic behaviour of a magma chamber depends on many factors including chamber geometry, physical properties of the magma and cooling history. Another important factor is where crystallization takes place; the possibilities being either along the floor, sides and roof of the chamber or within the magma. The evolution of a rectangular container with crystallization along the margins is considered below. These assumptions are unlikely to please all petrologists, but allow a simple description to be given and general principles to be illustrated. Natural systems will undoubtedly be much more complex and other kinds of processes, such as crystal settling, could become important. There is a vigorous debate at present on the relative importance of in-situ crystallization and crystal-settling in the evolution of basaltic magma chambers (Campbell 1978; McBirney and Noyes 1979; Morse 1979; Irvine 1980; Sparks et al. 1984). The consequences of these two different kinds of fractionation mechanism on the evolution of magma chambers are quite different. It is therefore considered worthwhile to explore magma chamber models in which marginal crystallization and convective fractionation are dominant.

The evolution of a closed-system magma chamber is described by considering all the magma to be at the primitive point P in Fig. 4. The magma begins to cool and fractionate by losing heat through the roof, sidewalls and floor of the chamber. The effect of the initial density decrease can be ascertained from laboratory experiments on the cooling from the margins of a container containing aqueous solutions whose saturation density decreases with decreasing temperature (Chen and Turner 1980; McBirney 1980; Turner 1980; Turner and Gustafson 1981). The details of the resulting fluid motions, the boundary layers and the crystallization will depend upon the exact conditions of the cooling and on the chamber geometry. However, the general conclusions to be drawn from all the experiments are that the lowest temperature, most differentiated magma will collect at the top of the chamber (Figs. 5a and b). A thermal and compositional stratification of the liquid can develop, with the hottest, least differentiated magma at the base overlain by relatively lighter and cooler, more differentiated magma (Fig. 5b). The stratification may not be as smooth as depicted in the figure; a series of steps may be expected

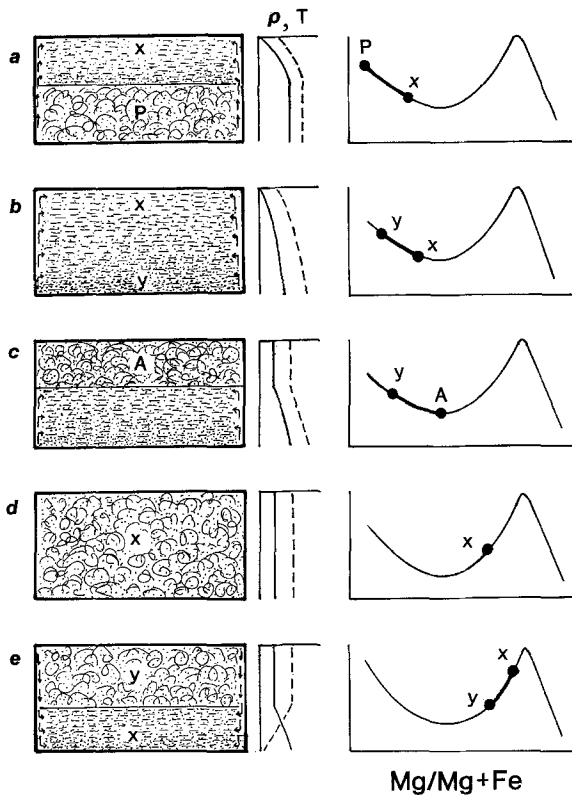


Fig. 5. Fluid dynamic models of the evolution of basaltic magma in a closed system. Schematic profiles of density (solid line) and temperature (dashed line) with height are shown for each model. The spread of compositions and densities for each model is indicated in schematic plots of density versus $(\text{Mg}/\text{Mg} + \text{Fe})$

reflecting compositional and thermal layering as seen in the laboratory experiments.

The rate at which liquid stratification develops depends both on chamber geometry (Chen and Turner 1980) and on where crystallization takes place. Sidewall cooling will be more important in comparison to cooling from the roof and floor in a chamber with a small width to depth ratio than in a chamber with a large width to depth ratio. The slope of the sidewalls also can influence the stratification rate. If the sidewalls dip outward or are vertical, boundary layer flows should form and move upwards adjacent to the walls. If the sidewalls or floor dip inward light fluid released by crystallization will detach from the boundary and rise into overlying magma and mix with it. Similarly, crystallization on the floor of the chamber will release light fluid that will mix convectively with overlying magma. In the case of bottom crystallization the lower well-mixed layer shown in Fig. 5a will not remain at composition P, but will become more differentiated. In this situation the well-mixed layer will decrease in density and will tend to inhibit the development of the overlying stratified region. Clearly there are some chamber geometries, in which crystallization is predominantly on the floor and a stratified region may only be poorly developed.

As the cooling and crystallization proceed, the density of the magma at any point in the interior of the chamber decreases. The temperature and density continue to decrease until sufficient heat has been lost for the magma at the top of the chamber to come to the minimum density point A on the curve of Fig. 4. Further loss of heat will

result in a layer of homogeneous temperature and composition corresponding to the density minimum point A being formed at the top of the chamber. The thickness of the layer will increase with time and pass through the state depicted in Fig. 5c. The zonation of the magma in the interior of the chamber is thus eradicated by encroachment from the top of the chamber by magma at the minimum density. This occurs because cooler magma, more differentiated than that at the minimum density, forming at the top of the chamber, would sink to its density level and mix to thermal equilibrium. By considering this process to occur in incremental steps a uniform layer can be shown to form. The thickness of the layer will increase until all the magma in the chamber, except possibly that in the boundary layers along the walls, top and bottom, comes to the temperature, composition and density of the minimum point A. If crystallization takes place on the floor and the density minimum A is reached, the residual fluid, being denser than overlying fluid, can remain at the bottom between the crystals.

An analogy to the situation shown in Fig. 5c is provided by some experiments carried out by Townsend (1964) on the natural convection in water over an ice surface. An interesting property of pure water is that the density has a maximum value at 4°C . In Townsend's experiments, a steady-state heat flow was established between a horizontal bottom surface of ice and an upper surface at 25°C . Production of cold water ($\sim 0^{\circ}\text{C}$) by melting the ice resulted in the formation of a well-mixed convecting region with a uniform temperature of 3.2°C beneath a statically stable, thermally stratified region. In both the water-ice system and in the magmatic system postulated here, adjacent well-mixed and stratified layers can form owing to the occurrence of maxima or minima in fluid density with changing temperature.

Thereafter, the interior will cool uniformly since the liquid density is now increasing as the temperature decreases. Dense magma generated at the roof drives convective mixing throughout the chamber and maintains the uniformity, whereas dense magma generated by crystallization on the floor remains stagnant (Fig. 5d).

Another process can become important, particularly if the sides or floors of the magma chamber are vertical or slope inwards to the centre (Fig. 5e). In this case cooling from the roof will continue to form well-mixed magma, but sidewall cooling will generate dense boundary layer flows of cool differentiated liquid which will collect at the base of the chamber. A stable stratified system will develop below a layer of hotter well-mixed magma. Double-diffusive layering can result from side-wall effects even if the vertical temperature and composition profiles are both stabilizing as depicted in Fig. 5e (Jacobs et al. 1981).

Evolution of replenished systems

At any point of the evolution described in the previous section, the chamber could be replenished by an input of new magma to the base. For simplicity the new magma is assumed to have the density and composition of point P on Fig. 4. The effects of this replenishment are described should it occur during any of the stages depicted in Fig. 5.

First, consider the case of replenishment at the base of the zoned system depicted in Fig. 5b or partly zoned system depicted in Fig. 5a. Because the input primitive

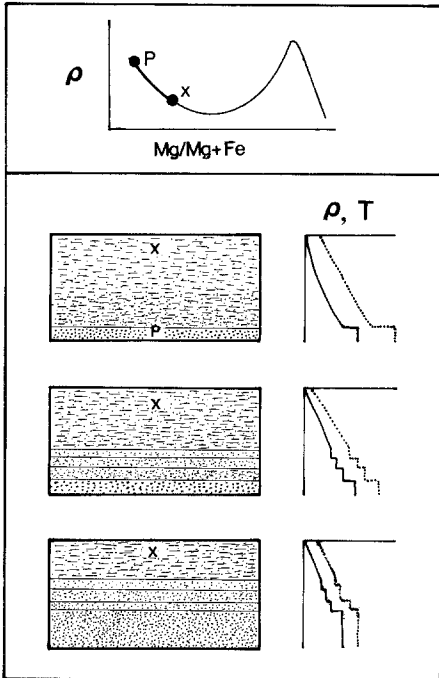


Fig. 6. Model for the replenishment of a compositionally stratified magma chamber by primitive magma. The range of composition, density and temperature are shown in schematic profiles

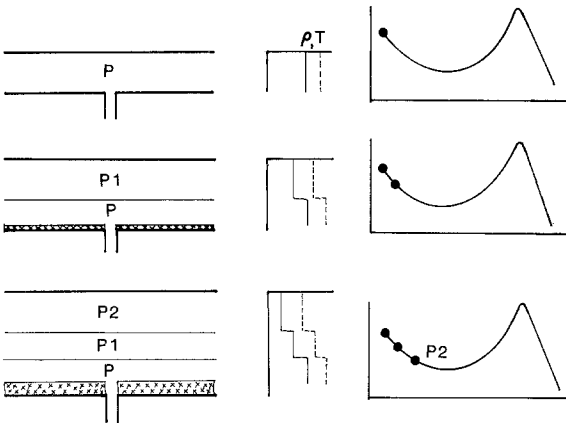


Fig. 7. Model for the formation of compositional and thermal stratification by replenishment. The layering in the chamber with accompanying schematic density and temperature profiles is shown after each of three successive replenishments

magma is denser than any of the resident magma, it ponds at the base of the chamber and cools predominantly by losing heat to the zoned magma above it (Fig. 6a). This is analogous to the experimental model of Huppert et al. (1982), using aqueous solutions. The gradient region can cool and evolve as described in the last section at the same time as the lowest layer cools and crystallizes (Fig. 6). When the lowest layer reaches the same temperature and density as the base of the gradient layer the magma layers will merge and mix together.

Replenishment offers an alternative mechanism to sidewall crystallization for the formation of stratification in a magma chamber. Figure 7 illustrates the essential principles in a one-dimensional chamber replenished by successive cycles of magma input. In the first cycle a homogeneous layer of primitive magma is emplaced and differentiates

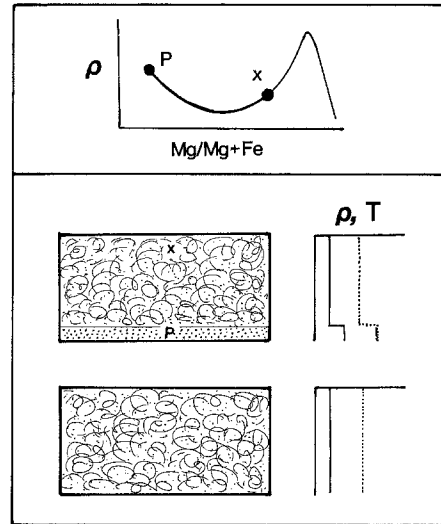


Fig. 8. Model for the replenishment by dense primitive magma of a well-mixed magma chamber containing plagioclase-saturated basalt

to composition and density P_1 . A new influx of magma of the primitive composition P is denser than P_1 and ponds beneath the first layer. Exchange of heat between P_1 and P would eventually result in the two layers merging because crystallization decreases the density of the lower layer despite the decrease in the temperature of the layer. However, before the thermal evolution of the system is complete another influx of composition P could form a third layer at the bottom of the chamber. Three layers of magma with compositions P , P_1 and P_2 are now present with stepwise changes in temperature through the chamber. If further cycles of primitive magma influx occur before the layers can reach thermal equilibrium a layered system can develop. Sidewall crystallization (Fig. 5a) and replenishment (Fig. 9) are competing mechanisms for producing compositional zonation, but it is not yet known which is quantitatively the most important in basaltic systems.

Next, consider the replenishment into a chamber filled entirely with a uniform magma, as depicted in Fig. 5d and Fig. 8. If the density of the input magma is greater than that in the chamber the influx will form a lower layer. The magma in this layer has only to evolve to a composition equal in density to the overlying evolved magma. At this stage the magma of the lower layer will rise and mix with that of the upper layer. The process has been modelled quantitatively by Huppert and Sparks (1980a, b), who explain how it leads to high temperature and low temperature cumulate layers with an abrupt transition from one type to another within each cyclic unit. This form of cyclic unit will be characterised by a lower ultramafic layer and an upper feldspar dominated layer separated by a sharp boundary.

The replenishment could take place after the resident magma has evolved sufficiently for its density to exceed that of the input. The new magma will then be relatively light and will immediately rise into the interior of the chamber (Fig. 11). It could rise as an entraining turbulent plume and mix rather thoroughly with the much larger volume of resident magma, as envisaged by Sparks et al. (1980). The new magma could rise through the chamber and form a layer of contaminated magma at the top, as

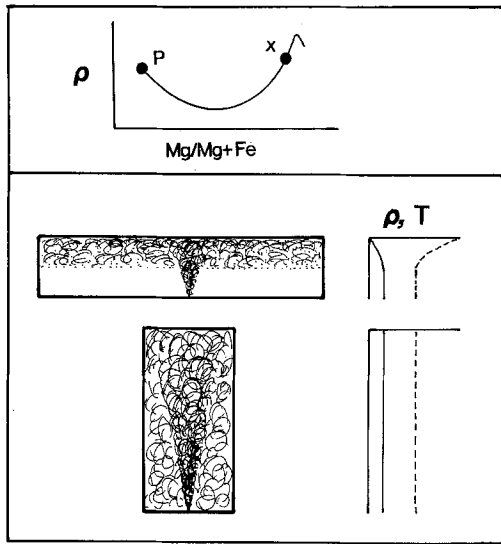


Fig. 9. Model for the replenishment of a well-mixed magma chamber by a light input of primitive magma

envisaged in the 'filling-box' model of Baines and Turner (1968). The aspect ratio of the chamber determines which will occur; thorough mixing occurs in chambers with large ratios of width to depth and formation of an upper layer in chambers with small ratios of width to depth.

Discussion

Laboratory and theoretical investigations of the fluid motions in crystallizing systems show that the rather small changes in density that occur during fractional crystallization have an important influence on the dynamic evolution of magma chambers. In order to understand these processes in natural systems it is necessary to know how the crystallization of different minerals affects melt density. The concept of fractionation density has been introduced, which allows an estimate to be made of the sign and magnitude of the density change during fractional crystallization without necessarily having to know the magma composition in great detail. The relative importance of compositional and temperature changes have been assessed during different stages of fractional crystallization. The data show that compositional effects are usually dominant.

The fractionation density parameter can be used to make some general deductions about density changes during differentiation. Fractionation of olivine and olivine plus pyroxene assemblages will cause magma density to decrease. It is not necessary to know the exact composition and density of the magma, since the fractionation density of such assemblages is considerably larger than the densities of basaltic magmas. In systems involving plagioclase crystallization as well as ferromagnesian minerals a number of useful deductions can be made using the data recorded in Table 2 and Fig. 3. Anhydrous tholeiitic basalts at mid-ocean ridges have densities ranging from 2.66 to 2.75 g cm⁻³ (Sparks et al. 1980). The commonest assemblages involved in their evolution are olivine-plagioclase and olivine-plagioclase-clinopyroxene. The fractionation density of olivine-plagioclase assemblages ranges from 2.64 to 2.70 g cm⁻³ (Fig. 3b) suggesting that such an assemblage can both decrease and increase magma density. On the other hand olivine-plagioclase-clinopyroxene assemblages

have fractionation densities which are significantly less than MORB and would therefore generally cause an increase in density. For MORB systems the density minimum (A in Fig. 4) can occur either when plagioclase joins olivine or can be delayed until pyroxene joins olivine and plagioclase.

The models for the evolution of basaltic magma chambers give a general conceptual framework for the development of an understanding of the dynamics of igneous differentiation. However, many of the basic processes in crystallizing systems are at present only understood in a qualitative way. The simple case of a dense hot layer of magma underlying a cold light layer is the only situation that has been modelled to a sufficient level of quantitative understanding to enable the time-scale and length-scales in a magma chamber to be calculated (Huppert and Sparks 1980b; Huppert and Turner 1981). Although the models in Figs. 5 to 9 are believed to be qualitatively correct there are several aspects of evolution which require further investigation. For example, the thicknesses of double-diffusive layers generated by heating a stratified chamber from below (Fig. 6) are not known yet. There is no quantitative understanding of how quickly magma chambers of various shapes and sizes become stratified by sidewall crystallization (Figs. 5a and 5b). Thus, in basaltic systems the relative importance of sidewall crystallization and replenishments as mechanisms for causing stratification has yet to be established.

Another area of uncertainty is the extent to which magma chambers crystallize at their roofs, floors and sides. As discussed in relation to Fig. 5, the location of crystallization and chamber geometry strongly affect whether stratification is developed or existing stratification is destroyed. For example, release of light liquid by crystallization on the floor or heavy liquid by crystallization on the roof can lead to convective mixing and destruction of stratification, whereas crystallization along sloping boundaries causes stratification to develop. Replenishment can likewise, depending on the circumstances, result in either formation of stratification (Fig. 7) or destruction of stratification. The balance between the various competing influences in a chamber will be hard to assess until quantitative models of the processes that have been identified are available.

This treatment has also ignored the important question of whether cumulates form by in-situ crystallization or by settling. Recent studies, particularly pertaining to the plagioclase density problem, have indicated that in-situ crystallization may be much more significant than previously supposed (e.g. Campbell 1978; McBirney and Noyes 1979; Morse 1979). In the case of in-situ crystallization against the roof, floor or margin the processes and principles outlined in this paper should apply. However, when crystallization occurs within the interior of the chamber, the bulk density of the magma will depart from the fractionation versus composition relationships like that depicted in Fig. 4. There are clearly many important aspects of magma chamber dynamics which require further investigation. Figures 5 to 9 are offered as a series of working hypotheses which do doubt will become modified as understanding improves.

Acknowledgments. We acknowledge the contribution of Stewart Turner to this study. Some of the important fluid dynamic processes invoked in this paper originated from his pioneering work

on the effects of crystallization on convection in fluids. We also thank Ian Campbell, Tim Druitt, Ross Kerr, Alex McBirney, Neil Irvine, Ian Parsons and Steve Tait for their constructive comments on earlier versions of the manuscript, although we have not always followed their advice. The following organisations and funds enabled the authors to visit the Research School of Earth Sciences, A.N.U., for several months where much of this manuscript was completed: The Anglo-Australasian Fellowship Scheme of the Royal Society, The Maurice Hill Fund and the Australian National University.

References

- Baines WD, Turner JS (1968) Turbulent buoyant convection from a source in a confined region. *J Fluid Mech* 37: 51–80
- Bender JF, Hodges FN, Bence PE (1978) Petrogenesis of the basalts from the project FAMOUS area. *Earth Planet Sci Lett* 41: 277–302
- Bottinga Y, Weill DF (1970) Densities of liquid silicate systems calculated from partial molar volumes of oxide components. *Am J Sci* 269: 169–182
- Bottinga Y, Weill DF, Richet P (1982) Density calculations for silicate liquids. I. Revised method for aluminosilicate compositions. *Geochim Cosmochim Acta* 46: 909–920
- Bryan WB (1979) Regional variation and petrogenesis of basalt glasses from the FAMOUS area, Mid-Atlantic Ridge. *J Petrol* 20: 293–325
- Campbell IH (1978) Some problems with cumulus theory. *Lithos* 11: 311–321
- Chen CF, Turner JS (1980) Crystallization in a double-diffusive system. *J Geophys Res* 85: 2573–2593
- Dane EB Jr (1941) Densities of molten rocks and minerals. *Am J Sci* 239: 809–821
- Fujii T, Kushiro I (1977) Density, viscosity and compressibility of basaltic liquid at high pressures. *Carnegie Inst Wash Yearb* 76: 419–424
- Grove TL, Gerlach DC, Sando TW (1982) Origin of calcalkaline lava series at Medicine Lake Volcano by fractionation, assimilation and mixing. *Contrib Mineral Petrol* 80: 160–182
- Huppert HE, Sparks RSJ (1980a) Restrictions on the compositions of mid-ocean ridge basalts: a fluid dynamical investigation. *Nature* 286: 46–48
- Huppert HE, Sparks RSJ (1980b) The fluid dynamics of a basaltic magma chamber replenished by influx of hot, dense ultrabasic magma. *Contrib Mineral Petrol* 75: 279–289
- Huppert HE, Sparks RSJ (1984) Double-diffusive convection due to crystallization in magmas. *Ann Rev Earth Planet Sci* 12: 11–37
- Huppert HE, Turner JS (1981) A laboratory model of a replenished magma chamber. *Earth Planet Sci Lett* 54: 144–152
- Huppert HE, Turner JS, Sparks RSJ (1982) Replenished magma chambers: effects of compositional zonation and input rates. *Earth Planet Sci Lett* 57: 345–357
- Irvine TN (1970) Crystallization sequences in the Muskox intrusion and other layered intrusions. *Geol Soc S Africa, Spec Pub* 1: 441–476
- Irvine TN (1980) Magmatic infiltration metasomatism, double-diffusive fractional crystallization and adcumulus growth in the Muskox intrusion and other layered intrusions. In: Hargreaves RB (ed) *Physics of Magmatic Processes*. Princeton University Press: 245–306
- Jacobs SS, Huppert HE, Holdsworth G, Drury DJ (1981) Thermohaline steps induced by melting of the Erebus glacier tongue. *J Geophys Res* 86: 6547–6555
- Kushiro I (1982) Density of tholeiitic and alkali basalt magmas at high pressures. *Carnegie Inst Wash Yearb* 81: 305–308
- McBirney AR (1980) Mixing and unmixing of magmas. *J Volcanol Geotherm Res* 7: 357–371
- McBirney AR, Noyes RM (1979) Crystallization and layering of the Skaergaard intrusion. *J Petrol* 20: 487–554
- McCullum IS, Raedeke LD, Mathez EA (1980) Investigations of the Stillwater Complex: Part I, Stratigraphy and structure of the banded zone. *Am J Sci* 280-A: 59–87
- Mo X, Carmichael ISE, Rivers M, Stebbins J (1982) Partial molar volume of Fe_2O_3 in multicomponent silicate liquids and the pressure dependence of oxygen fugacity in magmas. *Mineral Mag* 45: 237–245
- Morse SA (1969) The Kiglapait intrusion, Labrador. *Geol Soc Am Memoir* 112: 1–204
- Morse SA (1979) Kiglapait geochemistry I: Systematics, sampling and density. *J Petrol* 20: 555–590
- Murase T, McBirney AR (1973) Properties of some common igneous rocks and their melts at high temperatures. *Geol Soc Am Bull* 84: 3563–3592
- Nelson SA, Carmichael ISE (1979) Partial molar volume of oxide components in silicate liquids. *Contrib Mineral Petrol* 71: 117–124
- Presnall DC, Dixon JR, O'Donnell TM, Dixon SA (1979) Generation of mid-ocean ridge tholeiites. *J Petrol* 20: 3–36
- Sparks RSJ, Meyer P, Sigurdson H (1980) Density variation amongst mid-ocean ridge basalts: implications for magma mixing and the scarcity of primitive lavas. *Earth Planet Sci Lett* 46: 419–430
- Sparks RSJ, Huppert HE, Turner JS (1984) The fluid dynamics of evolving magma chambers. *Phil Trans Royal Soc (in press)*
- Stolper E, Walker D (1980) Melt density and the average composition of basalt. *Contrib Mineral Petrol* 74: 7–12
- Townsend AA (1964) Natural convection of water over an ice surface. *Q J Royal Met Soc* 90: 248–259
- Turner JS (1980) A fluid-dynamical model of differentiation and layering in magma chambers. *Nature* 285: 213–215
- Turner JS, Gustafson LB (1981) Fluid motions and compositional gradients produced by crystallization or melting at vertical boundaries. *J Volcanol Geotherm Res* 11: 93–125
- Walker D, Shibata T, Long SE (1979) Abyssal tholeiites from the Oceanographer Fracture Zone, II. Phase equilibria and mixing. *Contrib Mineral Petrol* 70: 111–125

Received December 13, 1982; Accepted November 11, 1983